Wave Interpretation of Numerical Results for the Vibration in Thin Conical Shells

Guangjian Ni

Institute of Sound and Vibration Research, University of Southampton, Highfield Campus, Southampton SO17 1BJ United Kingdom

G.Ni@soton.ac.uk

Stephen J. Elliott

Institute of Sound and Vibration Research, University of Southampton, Highfield Campus, Southampton SO17 1BJ United Kingdom

Abstract

The dynamic behaviour of thin conical shells can be analysed using a number of numerical methods. Although the overall vibration response of shells has been thoroughly studied using such methods, their physical insight is limited. The purpose of this paper is to interpret some of these numerical results in terms of waves, using the wave finite element, WFE, method. The forced response of a thin conical shell at different frequencies is first calculated using the dynamic stiffness matrix method. Then, a wave finite element analysis is used to calculate the wave properties of the shell, in terms of wave type and wavenumber, as a function of position along it. By decomposing the overall results from the dynamic stiffness matrix analysis, the responses of the shell can then be interpreted in terms of wave propagation. A simplified theoretical analysis of the waves in the thin conical shell is also presented in terms of the spatially-varying ring frequency, which provides a straightforward interpretation of the wave approach. The WFE method provides a way to study the types of wave that travel in thin conical shell structures and to decompose the response of the numerical models into the components due to each of these waves. In this way the insight provided by the wave approach allows us to analyse the significance of different waves in the overall response and study how they interact, in particular illustrating the conversion of one wave type into another along the length of the conical shell.

Key words: Conical shells; wave finite element; wave mode conversion

1 Introduction

Conical shell structures have been widely studied due to their extensive applications in engineering applications. In particular loudspeaker cones, which are a key element in determining the performance of moving coil loudspeakers, are often effectively modelled as conical shells[1, 2]. In order to study vibration patterns of the conical shell and carry out vibration control or dynamical design, it is necessary to understand the dynamics of conical shells. The study of the vibration in conical shells has a long history, which has been performed both analytically [3-5] and numerically [6-8] by many researchers. The conical shell under consideration here is a thin shell and could be described by a set of differential equations [5]. Some of the coefficients vary with position, however, which makes it difficult to solve those equations analytically. Some numerical techniques have been widely used in predicting natural frequencies, mode shape and forced response of conical shell. Raju *et al*. [6] used Novozhilov's strain-displacement relations for a conical shell to give the stiffness matrix for a finite element conical shell. Petyt and Gélat [8] derived the equations of motion of a cone and then used a Runge-Kutta approach to numerically obtain the dynamic stiffness matrix to analyse the dynamic response of the cone. Li *et al*. [3] employed Hamilton's principle with the Rayleigh-Ritz method to derive the equation of motion of the conical shell and obtained natural frequencies and the forced responses after solving the eigenvalue problem.

The dominant method of analysing the behaviour of conical shells such as loudspeaker cones is thus mostly numerical, often using the finite element or dynamic stiffness methods. These methods are often used to predict the natural frequencies and shapes of vibrating modes of the whole shell, when a loudspeaker "breaks up" at higher frequencies for example [8, 9].

Although there has been some effort to understand the dynamic behaviour of shells in terms of wave propagation, particularly for loudspeaker cones [1, 9], this approach has not been widely adopted. The object of the current paper is to demonstrate the way in which the results of a

dynamic stiffness approach to the prediction of thin conical shell dynamics can be interpreted in terms of waves, using the wave finite element method. This method is used to predict both the wavenumbers of the various waves that can contribute to the axisymmetric dynamics over a range of frequencies, and to decompose the results of a full dynamic stiffness matrix analysis at a single frequency into the components due to those waves.

The predictions of the wave finite element method are finally compared with the analytic work of Frankort [1] and Kaizer [9]. This results in an intuitively appealing description of the cone vibration as being either dominated by in-plane or out-of-plane waves at each axial position, with the transition being determined by the position-dependent local ring frequency.

2 Dynamics of Conical Shells

2.1 Equation of motion

We focus on thin conical shell which obeys the Kirchhoff-Love hypothesis [10]. The following assumptions are made for the thin conical shell:

1) Vibrations are axisymmetric.
2) The shell material is isotropic and obeys Hooke's law.
3) Displacements are small compared with the shell thickness (The displacements must be small. This linearizes the strain-displacement relations. The shell thickness comes into the picture only via the assumptions of Kirchhoff-Love, which put constraints on strains, but does not rule out large displacements).
4) Excitation is exerted on the inner boundary (small end).

Therefor the dynamic behaviour of a conical shell, with a geometry shown in Figure 1, can be calculated using thin shell theory [11]. The displacements and the internal forces of the conical shell median surface, as shown in Figure 1, can be related by six first-order differential equations as [5]

$$u' = -\upsilon\frac{u}{x} + \upsilon\frac{w}{x}\cot\alpha + \frac{\left(1-\upsilon^2\right)}{Eh}N_x, \tag{1}$$

$$w' = \theta, \tag{2}$$

$$\theta' = -\upsilon\frac{\theta}{x} + \frac{12\left(1-\upsilon^2\right)}{Eh^3}M_x, \tag{3}$$

$$N_x' = Eh\left(\frac{1}{x^2} - \frac{\rho\omega^2}{E}\right)u - Eh\frac{w}{x^2}\cot\alpha + \left(\frac{\upsilon-1}{x}\right)N_x, \tag{4}$$

$$Q_x' = -Eh\frac{\cot\alpha}{x^2}u - h\left(\frac{\cot^2\alpha}{x^2}E - \rho\omega^2\right)w - \upsilon\frac{\cot\alpha}{x}N_x - \frac{1}{x}Q_x, \tag{5}$$

$$M_x' = -\frac{Eh^3}{12x^2}\theta - Q_x + \frac{\left(\upsilon-1\right)}{x}M_x, \tag{6}$$

where x is the position along the cone meridian, α is the half angle of the conical shell, u is the displacement along the meridian (positive in the direction of positive x), w is the displacement normal to the meridian (positive inward) and θ is the rotation about the cone meridian, x, as shown in Figure 1, N_x is the membrane force in the direction of the meridian (positive in the direction of positive x), Q_x is the normal shearing force (positive outwards normal to the meridian) and M_x is the bending moment in the circumferential direction (all per unit length of mid-plane in the circumferential direction, and is positive in a counter-clockwise direction along the positive x). E is Young's modulus of the shell material, h is the shell thickness, υ is Poisson's ratio, ρ is the density of shell material and ω is angular frequency.

Equations (1) to (6) are presented in a form which is convenient for numerical integration. The equations are valid not only for uniform shells but also for those with varying thickness and material properties along the direction of meridian. In the case considered here, however, the shell material is assumed to be isotropic for illustrating purpose. Equations (1) to (6) are linear, ordinary differential equations with variable coefficients and have no known analytic solutions

[8]. So numerical approaches, such as the dynamic stiffness method (DSM) [8], provide an efficient way to relate the forces and displacements of the conical shell.

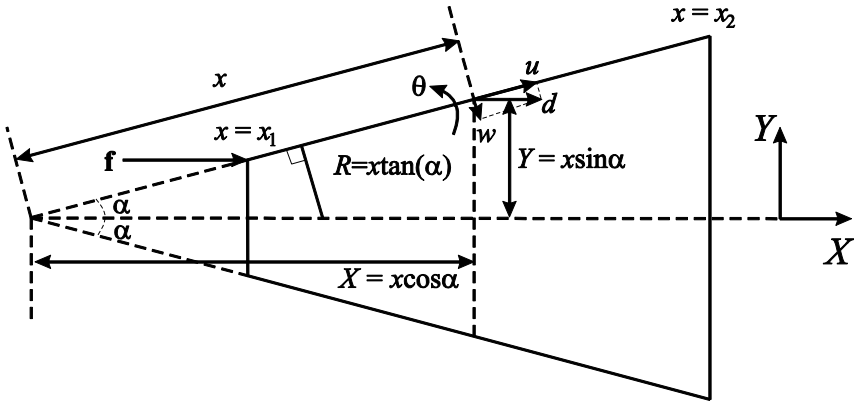

Figure 1 Side view of the conical shell in local coordinates, x denotes position along the cone meridian, X and Y are the axial and radial positions in the global coordinates, α is the angle between the axis and meridian.

Equations (1) to (6) can be written in "state space" form as [8]

$$\frac{\partial \mathbf{y}(x)}{\partial x} = \mathbf{A}(x)\mathbf{y}(x), \tag{7}$$

where

$$\mathbf{y}(x) = \begin{bmatrix} u \\ w \\ \theta \\ N_x \\ Q_x \\ M_x \end{bmatrix}, \tag{8}$$

and

$$\mathbf{A}(x)=\begin{bmatrix} -\frac{\upsilon}{x} & \frac{\upsilon\cot\alpha}{x} & 0 & \frac{\left(1-\upsilon^2\right)}{Eh} & 0 & 0 \\ 0 & 0 & 1 & 0 & 0 & 0 \\ 0 & 0 & -\frac{\upsilon}{x} & 0 & 0 & \frac{12\left(1-\upsilon^2\right)}{Eh^3} \\ Eh\left(\frac{1}{x^2}-\frac{\rho\omega^2}{E}\right) & -\frac{Eh\cot\alpha}{x^2} & 0 & \left(\frac{\upsilon-1}{x}\right) & 0 & 0 \\ -\frac{Eh\cot\alpha}{x^2} & -h\left(\frac{\cot^2\alpha}{x^2}E-\rho\omega^2\right) & 0 & -\frac{\upsilon\cot\alpha}{x} & -\frac{1}{x} & 0 \\ 0 & 0 & -\frac{Eh^3}{12x^2} & 0 & -1 & \frac{\left(\upsilon-1\right)}{x} \end{bmatrix}. \tag{9}$$

The relationship between the nodal forces and the nodal displacements at two arbitrary positions along the conical shell can be characterised by a dynamic stiffness matrix, **D**, as

$$\mathbf{Dq}=\mathbf{f}, \tag{10}$$

where **q** is the vector of displacements including u, w, and θ and **f** is the corresponding vector of forces N_x, M_x and Q_x. Based on equation (7), the dynamic stiffness matrix of the shell can be calculated by the Runge-Kutta approximation [8]. The accuracy of the model depends mainly upon the step size used in the Runge-Kutta analysis, rather than the number of segments, as defined in Figure 3, which the conical shell has been discretized into.

2.2 Forced responses

As a numerical example, the forced response of a uniform straight conical shell, whose geometry and material properties are listed in Table 1, is predicted here using the DSM [8], with 512 elements and a step size of 0.1 mm, when excitation is applied axially at the inner edge. The boundary conditions of the conical shell are free at the outer end and the conical shell is only allowed to move along its meridian at the inner edge. Damping is included in the shell by introducing a loss factor to define a complex Young's modulus. The complex Young's modulus then becomes $E(1+i\eta)$, where η is the loss factor.

Table 1 Assumed properties of the conical shell.

Parameter	Unit	Value
Cone angle α	rad	$2\pi/9$
Cone length L	m	0.108
Initial value on the X axis	m	0.0209
Young's modulus E	Pa	1.5×10^{9}
Density ρ	kg/m^3	900
Loss factor η	-	0.02
Poisson's ratio v	-	0.33
Thickness h	m	0.5×10^{-3}

A harmonic force *f*, whose dependence on $e^{i\omega t}$ is suppressed here for brevity, is applied uniformly over the circumference of the conical shell's inner edge in the axial direction. The forced response is calculated at different frequencies and instantaneous snapshots of the resulting vibration patterns are shown in Figure 2. Different forces are applied for different driving frequencies in order to show clearly the difference between the deformation and the un-deformed surface. The dashed lines in each subfigure stand for the un-deformed middle surfaces and the solid lines denote the deformed middle surfaces.

It can be seen that at low frequency, 100 Hz for example, the conical shell moves as a rigid body, and the amplitude of motion in the axial direction, *X*, is much greater than that in the radial direction, *Y*. Also, the real part of the displacement in the axial direction is much greater than its imaginary part and is constant along the axis. The amplitude of this displacement, *d*, of the conical shell of mass *m* under a harmonic force of magnitude *f* and frequency ω is closely given by $d = -f/m\omega^2$, based on Newton's Second Law of Motion. The difference between the numerical predication and that using Newton's Second Law of Motion is less than 1% at 100 Hz.

At higher frequencies, 2 kHz and 3 kHz, "break-up" occurs, in which the conical shell no longer vibrates as a whole, but some parts of the shell still move in phase. In this frequency range, the

conical shell vibration is dominated by bending in the region on the outer part of the shell. The position, called the “transition point”, where the bending wave begins, moves towards the inner edge as driving frequency increases. At 10 kHz driving frequency, the whole conical shell moves with a bending motion.

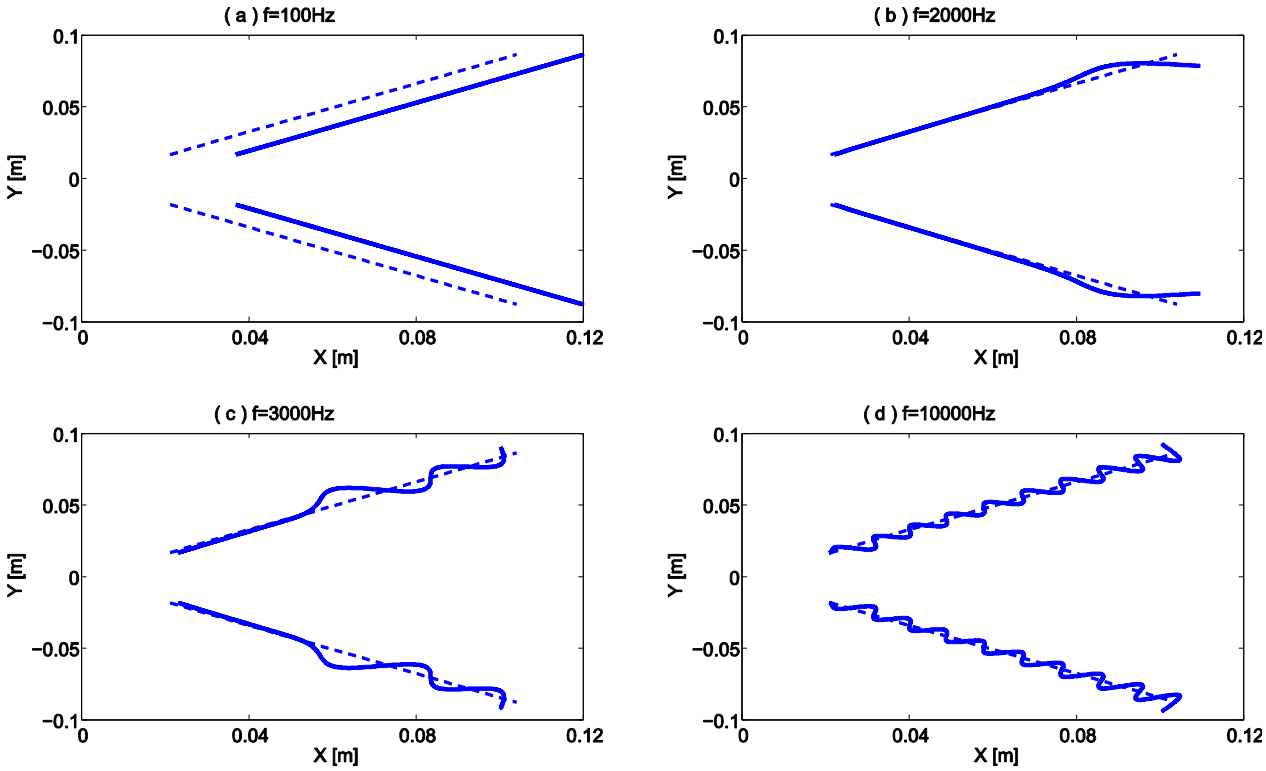

Figure 2 Snap shots of forced responses of the straight conical shell at (a) 100 Hz, (b) 2 kHz, (c) 3 kHz and (d) 10 kHz predicted using the dynamic stiffness matrix method. The displacements are plotted in the global coordinates denoted by solid line and the un-deformed middle surface of the shell is represented by dashed line.

3 Waves in a conical shell

Numerical approaches such as the dynamic stiffness matrix method and the finite element method are convenient to predict the overall response of conical shells, but they lack physical insight. In order to provide a greater degree of physical insight, the results of the numerical prediction can be interpreted in terms of waves. The types of waves that can propagate in an element of a thin conical shell are predicted here using the wave finite element method, which can then be used to decompose the results of the full numerical model into wave components.

3.1 Wave finite element method

The WFE method is a numerical approach to investigate wave motion in waveguides and slender structures at low computational cost [12-16]. The WFE method starts by first modelling a short segment, as shown in Figure 3, of the conical shell using a conventional method, such as the Dynamic Stiffness method or the Finite Element method, so that the equation of motion is defined in terms of a finite number of degrees of freedom, DOFs, in order to find the dynamic stiffness matrix. The transfer matrix of the segment is then formed using elements of the dynamic stiffness matrix, and finally, the eigenvalues and eigenvectors of the transfer matrix, which represent the free wave propagation characteristics such as the wavenumbers and wave modes, are obtained from solving the eigenvalue problem of the transfer matrix after applying periodicity conditions [14, 15].

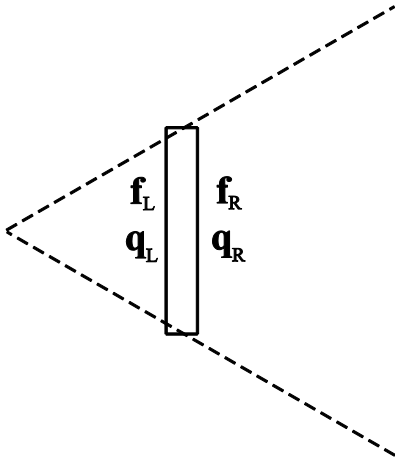

Figure 3 A segment of a thin conical shell.

Here we take a short section, which is assumed to be uniform, of the conical shell and express all the internal complex forces, at a given excitation frequency, as a function of all the complex displacements multiplied by the corresponding dynamic stiffness obtained in the previous forced response analysis. The vector of these internal forces and displacements is then partitioned into those on the left and right hand side of the *n*-th segment of the conical shell, so that

$$\begin{bmatrix} \mathbf{D}_{\mathrm{LL}}(n) & \mathbf{D}_{\mathrm{LR}}(n) \\ \mathbf{D}_{\mathrm{RL}}(n) & \mathbf{D}_{\mathrm{RR}}(n) \end{bmatrix} \begin{bmatrix} \mathbf{q}_{\mathrm{L}}(n) \\ \mathbf{q}_{\mathrm{R}}(n) \end{bmatrix} = \begin{bmatrix} \mathbf{f}_{\mathrm{L}}(n) \\ \mathbf{f}_{\mathrm{R}}(n) \end{bmatrix}, \tag{11}$$

where the subscripts L and R represent the displacement and forcing vector on the left and right hand side of the *n*-th segment. The terms in equation (11) can be re-arranged to express the forces and displacements on one side of the segment in terms of those on the other side, as

$$\begin{bmatrix} \mathbf{q}_{\mathrm{R}}(n) \\ -\mathbf{f}_{\mathrm{R}}(n) \end{bmatrix} = \mathbf{T}(n) \begin{bmatrix} \mathbf{q}_{\mathrm{L}}(n) \\ \mathbf{f}_{\mathrm{L}}(n) \end{bmatrix}, \tag{12}$$

where $\mathbf{T}(n)$ is the transfer matrix of the *n*-th segment and can be expressed in terms of the dynamic stiffness as [14]

$$\mathbf{T}(n) = \begin{bmatrix} -\mathbf{D}_{\mathrm{LR}}^{-1}(n)\mathbf{D}_{\mathrm{LL}}(n) & \mathbf{D}_{\mathrm{LR}}^{-1}(n) \\ -\mathbf{D}_{\mathrm{RL}}(n) + \mathbf{D}_{\mathrm{RR}}(n)\mathbf{D}_{\mathrm{LR}}^{-1}(n)\mathbf{D}_{\mathrm{LL}}(n) & -\mathbf{D}_{\mathrm{RR}}(n)\mathbf{D}_{\mathrm{LR}}^{-1}(n) \end{bmatrix}. \tag{13}$$

Sometimes, the inversion of matrix may cause numerical errors if the matrix is ill-conditioned, however, Zhong [12, 17] has suggested an approach to reformulate the eigenvalue problem with better matrix conditioning. The numerical issues involved with the wave finite method are also discussed by Waki *et al.*[18].

Assuming the dynamics only change a little from one element to the next, a particular vibrating pattern of displacements and forces, due to the *m*-th wave, on the right hand side of the segment is equal to the same pattern on the left hand side of the segment, multiplied by a complex constant of proportionality λ_m, so that

$$\begin{bmatrix} \mathbf{q}_{\mathrm{R}}(n,m) \\ -\mathbf{f}_{\mathrm{R}}(n,m) \end{bmatrix} = \lambda_m \begin{bmatrix} \mathbf{q}_{\mathrm{L}}(n,m) \\ \mathbf{f}_{\mathrm{L}}(n,m) \end{bmatrix}. \tag{14}$$

This vibration pattern then would travel as a propagating, evanescent or oscillating wave along the cone with a complex wavenumber, k_m, determined by

$$\lambda_m = e^{-ik_m\Delta}, \tag{15}$$

where Δ is the length of the cone segment and the type of wave depends on the relative magnitude of the real and imaginary parts of the wavenumber. The right hand side of equation (12) must now be equal to the right hand side of equation (14), and so λ_m, and the corresponding distribution of

displacements and forces, must be an eigenvalue, and the corresponding eigenvector, of the transfer matrix for this segment. The wavenumber is assumed not to vary too greatly within segment, so that $k_m\Delta$ is very small compared with unity [18].

3.2 Wavenumber distributions

The wavenumber can be obtained directly from solving the eigenvalue problem for the transfer matrix **T**(*n*). Figure 4 shows the distribution of the real and imaginary parts of the wavenumber along the conical shell axis for an excitation frequency of 3000 Hz. Since each of the 512 segments of the conical shell has 3 degrees of freedom, DoFs, on each face of the cone segment, there are 3 pairs of eigenvalues for the transfer matrix **T**(*n*) of each segment. One half of these pairs, whose imaginary part is negative, are forward-going waves. We can divide the behaviour of waves into 2 regions separating by a transition point, which corresponds to about 3 kHz in this example, along the shell axis, as shown in Figure 4. Region A includes inner end to the transition point at about 0.06 m and region B corresponds to from 0.06 m to the outer edge of the conical shell. It can be seen that not all waves can propagate along the shell in region A, since they have non-zero imaginary wavenumber indicating they are oscillating and decaying. Specifically, wave 1, associated with the DoF *u*, propagates with a gradually decreasing speed and decays less than the other two waves, since wave 1 has a small non-zero imaginary part of wavenumber. In this example, the phase velocities of wave 1 and 2 are 1069 m/s and 769.9 m/s at 0.04 m and 19922 m/s and 77.1 m/s at 0.08 m in the shell *X* direction at 3000 Hz. This shows that in the region A, the longitudinal motion dominates the vibration pattern of the cone. Beyond the position 0.06 m, wave 2, associated with DoFs *w* and θ, starts to propagate towards the outer edge. Wave 1 becomes an evanescent wave beyond the position 0.06 m. Wave 3, also associated with DoFs *w* and θ, has a large non-zero imaginary part of wavenumber along the whole range of the conical shell, which indicates that this wave is evanescent along the whole conical shell length.

Although we can find the properties of each wave from the wavenumber variations, the contribution of each wave to the overall vibration of the conical shell cannot be directly seen from this analysis. So the forced response from the previous analysis is now decomposed into wave components, which can show the contribution of each wave to the overall vibration.

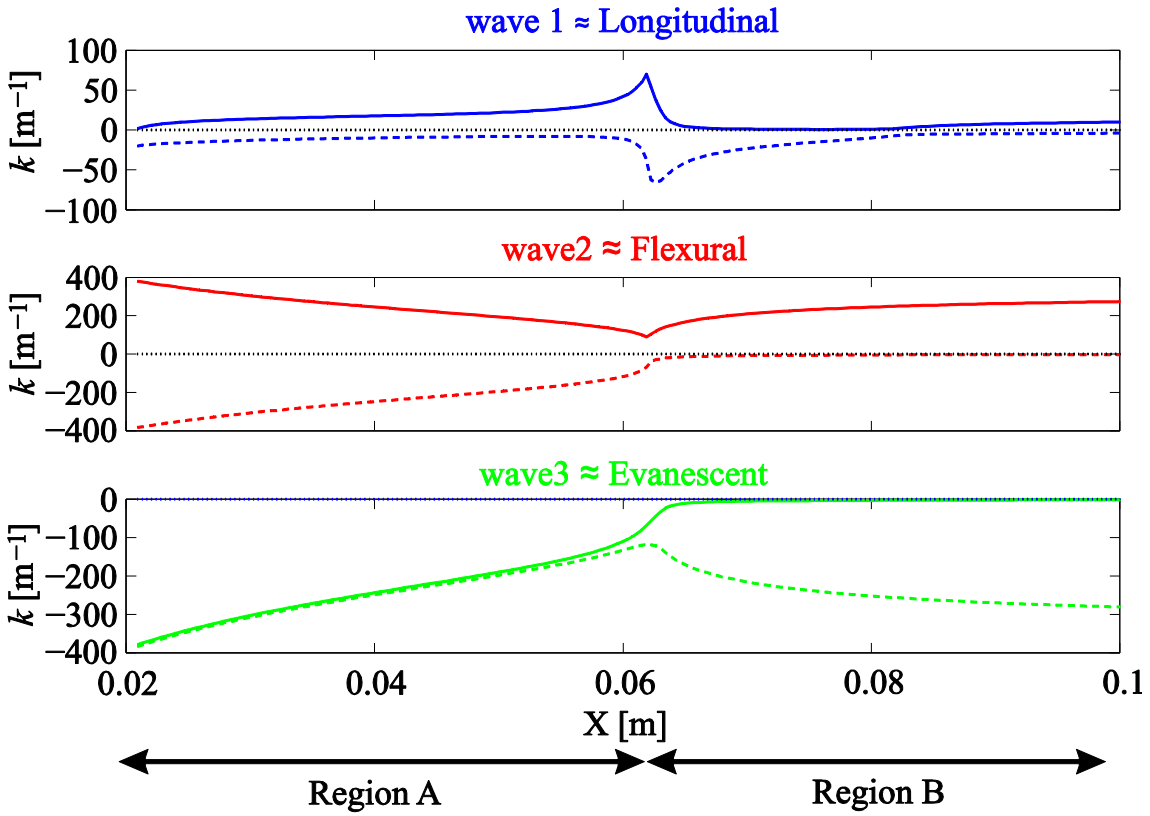

Figure 4 Wavenumber distribution along the conical shell axis at 3 kHz using the WFE, with only wavenumbers corresponding to forward-going waves plotted, and solid lines being the real component of the wavenumber k, and dashed lines being the imaginary component (color online).

4 Decomposition into wave components

In general, the transfer matrix $\mathbf{T}$ has a size of $N \times N$ and has a linearly independent set of N eigenvectors. Thus we can express the eigenvalue, eigenvector decomposition of the transfer matrix for the n-th segment in the form

$$\mathbf{T}(n) = \mathbf{Q}(n)\mathbf{\Lambda}(n)\mathbf{Q}^{-1}(n), \tag{16}$$

where $\mathbf{\Lambda}(n)$ is the diagonal matrix of eigenvalues, the columns of $\mathbf{Q}(n)$ are the right eigenvectors of $\mathbf{T}(n)$ and the rows of $\mathbf{Q}^{-1}(n)$ are the left eigenvectors of $\mathbf{T}(n)$.

Using equation (16), equation (12) can also be written as [19]

$$\mathbf{Q}^{-1}(n)\begin{bmatrix}\mathbf{q}_{\mathrm{R}}(n)\\ -\mathbf{f}_{\mathrm{R}}(n)\end{bmatrix}=\mathbf{\Lambda}(n)\mathbf{Q}^{-1}(n)\begin{bmatrix}\mathbf{q}_{\mathrm{L}}(n)\\ \mathbf{f}_{\mathrm{L}}(n)\end{bmatrix}. \tag{17}$$

Since $\mathbf{\Lambda}(n)$ is diagonal, the inner product of each row of $\mathbf{Q}^{-1}(n)$, which is a left eigenvector of $\mathbf{T}(n)$, with the "state vectors" on the right and left hand side gives an equation of the form

$$a_{\mathrm{R}m}(n)=\lambda_m(n)a_{\mathrm{L}m}(n), \tag{18}$$

where $a_{\mathrm{R}m}(n)$ and $a_{\mathrm{L}m}(n)$ can be interpreted as the complex amplitudes of the *m*-th wave on the right and left hand side of the *n*-th segment [15]. The vector of all such wave amplitudes, on the right hand side of this segment, for example, can be written as

$$\mathbf{a}_{\mathrm{R}}(n)=\mathbf{Q}^{-1}(n)\begin{bmatrix}\mathbf{q}_{\mathrm{R}}(n)\\ -\mathbf{f}_{\mathrm{R}}(n)\end{bmatrix}. \tag{19}$$

The axial displacement, $d(n,m)$, due to the *m*-th wave at the *n*-th position is given by

$$d(n,m)=\mathbf{sq}(n,m)a(n,m), \tag{20}$$

where $\mathbf{s}$ is the weighting vector, $\mathbf{s}=[\cos\alpha\ \sin\alpha]$, $\mathbf{q}(n,m)$ is the displacement vector for the *m*-th wave at the *n*-th position and $a(n,m)$ is the wave amplitude for the *m*-th wave at the *n*-th position. The contributions to the axial displacement distributions, calculated using the DSM method, due to each of the forward going waves shown in Figure 4, are plotted in Figure 5.

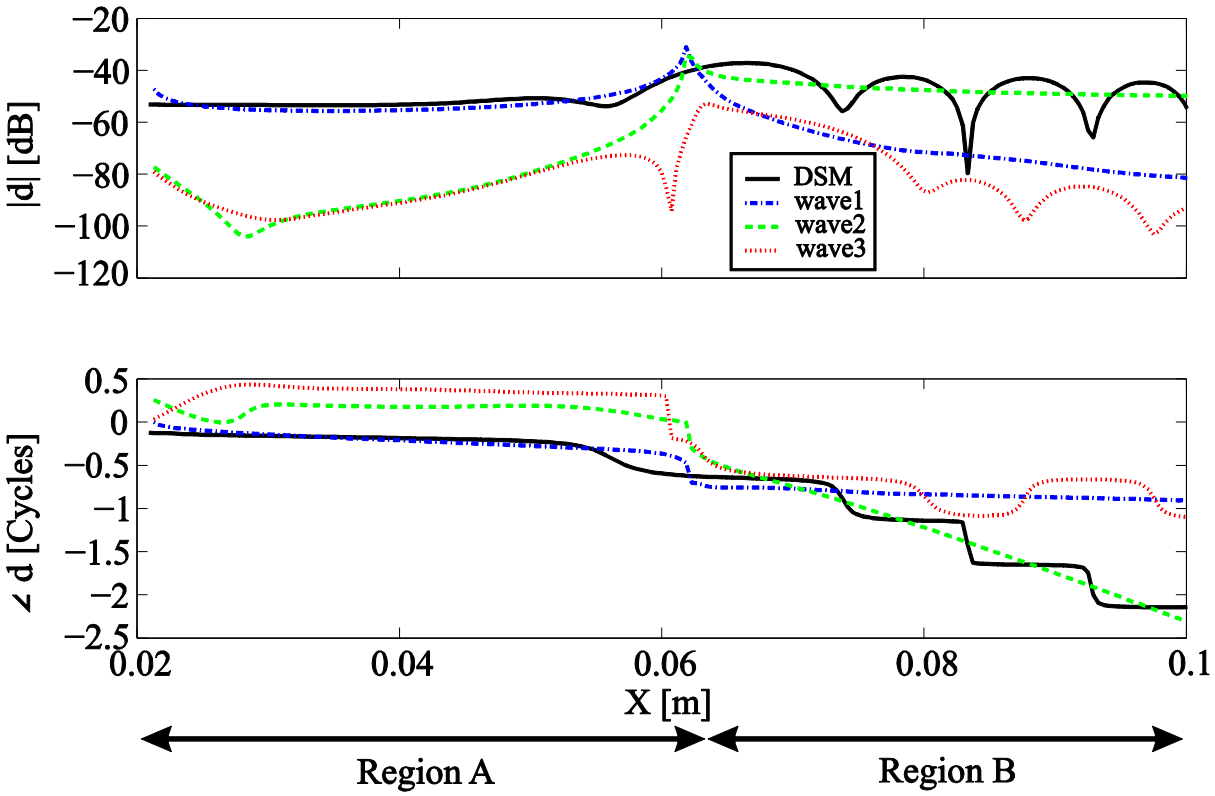

Figure 5 Decomposition of the overall axial displacement calculated from the DSM model into components due to forward-going waves in Figure 4, calculated from the wave finite element model.

The contribution of wave 1 is seen to be in reasonable agreement with the overall result from the DSM method for positions in region A. In region B, the contribution of wave 1 is significantly less than the overall result of the DSM for positions beyond the peak response, the contribution of wave 2, however, dominates the overall response. There is also a negative-going component of wave 2, which has the same real and imaginary parts of wavenumber with wave 2 but has opposite sign, due to the reflection from the free outer edge of the conical shell. The interference between the negative-going and the forward-going flexural wave gives rise to the standing wave like pattern seen in the DSM results. The contribution of wave 3 decays away on either side of this peak, and the amplitude is too small to significantly affect the overall response. In region A the wavelength is long, due to the predominance of longitudinal motion, and in region B the wavelength is much shorter, due to the predominance of bending motion. The vibrational energy in the shell is converted from longitudinal motion to bending motion at the transition point.

5 Ring Frequency Analysis of Conical Shells

The dynamic behaviour at a given position along the conical shell can be analysed depending on whether the excitation is above or below the ring frequency, f_r , at this location [20]. The ring frequency is given by

$$f_r = \frac{c}{2\pi R}, \tag{21}$$

where c is the speed of longitudinal waves, determined by Young's modulus E and material density ρ as $\sqrt{E/\rho}$, R is the distance between the conical shell and conical shell axis measured perpendicular to the conical shell meridian. The ring frequency is plotted for the conical shell with assumed parameters listed in Table 1, in Figure 6. Below the ring frequency the dynamics are dominated by the membrane stiffness, resulting in mostly in-plane, longitudinal, motion. Above the ring frequency the dynamics are dominated by the bending stiffness, resulting in out-of-plane, transverse, motion. Since the ring frequency varies along the length of the conical shell, however, the dynamic behaviour of the structure depends on whether the frequency is in one of the three regions, as shown in Figure 6. In region I, the excitation frequency is below the ring frequency at every position along the conical shell, so the structure moves entirely in phase as a quasi-rigid body, as shown in Figure 2 (a). In region II, the excitation frequency is below the ring frequency at the inner edge but above it at the outer edge, so that part of the conical shell is still moving as a quasi-rigid body and part of it has "broken up" into transverse motion. In region III, the excitation frequency is above the ring frequency all along the conical shell, so the dynamics are dominated by bending waves at all positions. For example, when the excitation frequency is 3000 Hz, which locates in region II, wave 2 (bending wave) starts propagating and dominating the overall behaviour beyond the position 0.06 m, as shown in Figure 4 and Figure 5. This position is about 0.6 of the whole length of the cone, as shown in Figure 6.

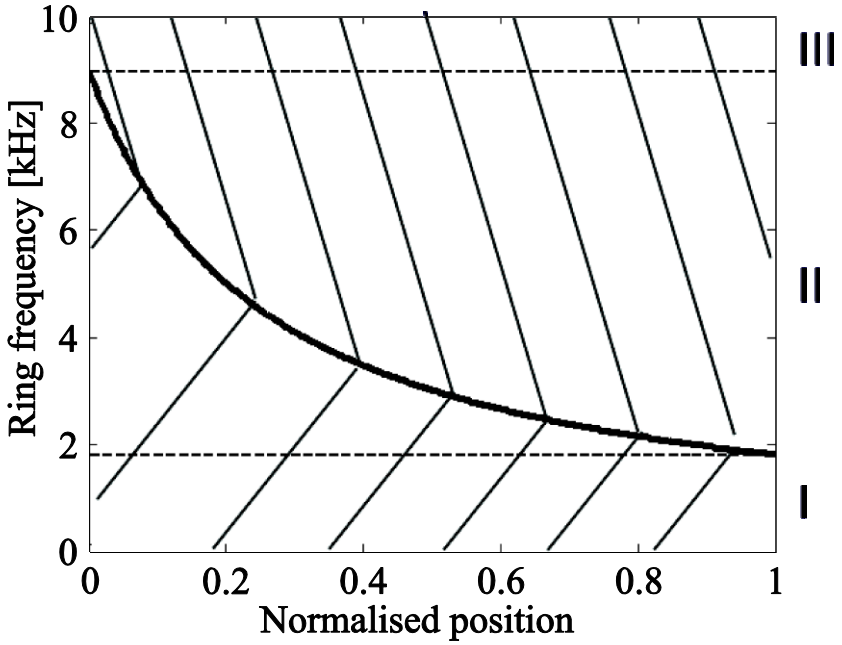

Figure 6 The ring frequency as a function of position along the conical shell meridian indicating the transition between mostly in-plane (///) and mostly out-of-plane (\\\) behaviour.

At low frequencies, the conical shell can be well approximated by a rigid piston. For loudspeaker cones, the diaphragm can be assumed to be rigid and move as a unit without deformation at low frequency [5]. This rigid piston model is the simplest model for calculating the sound radiation of a loudspeaker cone, since at low frequencies the wavelength in air λ_0 is much greater than the cone dimensions. In this case, the radiation of cone and piston move in a similar way and the cone can be modelled as an acoustic point source.

However, the conical shell is not rigid at high frequencies and must be modelled as a flexible system [1]. When the driving frequency increases above a certain frequency, indicated by the transition from region I to region II in Figure 6, the cone begins to break up and the acoustic wavelength λ_0 is generally large compared with the wavelength of the bending waves on the cone, so region II does not result in strong radiation.

The effective acoustic dimension of the loudspeaker is thus reduced with increasing frequency, reducing the beaming at high frequencies.

6 Conclusion

The vibration of the conical shell has previously been well studied using numerical methods, such as the Dynamic Stiffness Method, Finite Element Method etc., but these methods only predict the overall dynamic behaviour, without any physical interpretation in terms of wave propagation. This paper combines a conventional numerical method, DSM, and the wave finite element method to study waves in a conical shell and the decomposition of the results from the DSM model into wave components, in order to illustrate the contribution of each wave to the overall response. The overall response of the conical shell considered here results from a coupling between longitudinal and bending motion. At an excitation frequency of 3000 Hz, for example, the longitudinal motion plays a major part in the response from the inner edge to a transition point some way along the cone, but the bending motion dominates the overall response beyond this region. This behaviour is readily illustrated in the case of a uniform straight cone by considering the change of ring frequency with position [20].

More generally, however, the wave finite element method provides a method of studying the types of wave that can travel in a conical shell and, more importantly, decomposing the overall response of a numerical model into the components due to each of these waves. This illustrates the vibration wave mode conversion that occurs from longitudinal to bending waves along the length of the cone. In this way the insight provided by the wave approach can be brought to bear on the numerical models, even for those with more complicated structures.

Acknowledgement

We would like to thank Dr. A. Langley for his helpful discussion and suggestion.

References

[1] F.J.M. Frankort, Vibration and sound radiation of loudspeaker cones, in: Philips Research Report. Supplements No. 2, Philips Research Laboratories, Eindhoven, 1975, pp. 1-189.
[2] F.J.M. Frankort, Vibration patterns and radiation behavior of loudspeaker cones, The Journal of the Audio Engineering Society, 26 (1978) 609-622.
[3] F. Li, K. Kishimoto, W. Huang, The calculations of natural frequencies and forced vibration responses of conical shell using the Rayleigh–Ritz method, Mechanics Research Communications, 36 (2009) 595-602.
[4] M. Caresta, N.J. Kessissoglou, Free vibrational characteristics of isotropic coupled cylindrical–conical shells, Journal of Sound and Vibration, 329 (2010) 733-751.
[5] J.E. Goldberg, J.L. Bogdanoff, L. Marcus, On the calculation of the axisymmetric modes and frequencies of conical shells, The Journal of the Acoustical Society of America, 32 (1960) 738-742.
[6] I.S. Raju, G.V. Rao, B.P. Rao, J. Venkataramana, A conical shell finite element, Computers & Structures, 4 (1974) 901-915.
[7] D.P. Thambiratnam, Y. Zhuge, Axisymmetric free vibration analysis of conical shells, Engineering Structures, 15 (1993) 83-89.
[8] M. Petyt, P.N. Gélat, Vibration of loudspeaker cones using the dynamic stiffness method, Applied Acoustics, 53 (1998) 313-332.
[9] A.J.M. Kaizer, Theory and numerical calculation of the vibration and sound radiation of non-rigid loudspeaker cones, in: Philips Internal Report, Philips Research Laboratories, Eindhoven, 1979.
[10] E.H. Baker, L. Kovalevsky, F.L. Rish, Structural Analysis of Shells, McGraw-Hill, 1972.
[11] A.W. Leissa, Vibration of shells, American Institute of Physics for the Acoustical Society of America, New York, 1993.
[12] W.X. Zhong, F.W. Williams, On the direct solution of wave propagation for repetitive structures, Journal of Sound and Vibration, 181 (1995) 485-501.
[13] L. Houillon, M.N. Ichchou, L. Jezequel, Wave motion in thin-walled structures, Journal of Sound and Vibration, 281 (2005) 483-507.
[14] B.R. Mace, D. Duhamel, M.J. Brennan, L. Hinke, Finite element prediction of wave motion in structural waveguides, The Journal of the Acoustical Society of America, 117 (2005) 2835-2843.
[15] D. Duhamel, B.R. Mace, M.J. Brennan, Finite element analysis of the vibrations of waveguides and periodic structures, Journal of Sound and Vibration, 294 (2006) 205-220.
[16] D. Chronopoulos, B. Troclet, O. Bareille, M. Ichchou, Modeling the response of composite panels by a dynamic stiffness approach, Composite Structures, 96 (2013) 111-120.
[17] W. Zhong, J. Lin, C. Qiu, Eigenproblem of substructure chain and the expansion solution, Acta Mechanica Sinica, 7 (1991) 169-177.
[18] Y. Waki, B.R. Mace, M.J. Brennan, Numerical issues concerning the wave and finite element method for free and forced vibrations of waveguides, Journal of Sound and Vibration, 327 (2009) 92-108.
[19] S.J. Elliott, G. Ni, B.R. Mace, B. Lineton, A wave finite element analysis of the passive cochlea, The Journal of the Acoustical Society of America, 133 (2013) 1535-1545.
[20] A.J.M. Kaizer, Theory and numerical calculation of the vibration and sound radiation of non-rigid loudspeaker cones, in: 62nd Convention of the Audio Engineering Society AES, Brussels, paper number 1437, 1979.